ADVANCES IN ATMOSPHERIC SCIENCES, VOL. 27, NO. 5, 2010, 1043–1050

Seasonality of Interannual Inter-hemispheric Oscillations over the Past Five Decades

GUAN Zhaoyong* (管兆勇), LU Chuhan[1] (卢楚翰), MEI Shilong[2] (梅士龙), and CONG Jing[3] (丛 菁)

[1] *Key Laboratory of Meteorological Disaster of Ministry of Education, College of Atmospheric Sciences, Nanjing University of Information Science and Technology, Nanjing* 210044

[2] *Weather Service Division of Jiaxing Meteorological Bureau, Jiaxing* 314000

[3] *Dalian Municipal Meteorological Bureau, Dalian* 116001

(Received 21 July 2009; revised 1 December 2009)

ABSTRACT

Air mass is inter-hemispherically redistributed, leading to an interesting phenomenon known as the Inter-Hemispheric Oscillation (IHO). In the present article, the seasonality of the interannual IHO has been examined by employing monthly mean reanalyses from NCEP/NCAR, EAR40, and JRA25 for the period of 1958–2006. It is found that the IHO indices as calculated from different reanalyses are generally consistent with each other. A distinct seesaw structure in all four seasons between the northern and southern hemispheres is observed as the IHO signature in both the surface air pressure anomalies (SAPAs) and the leading EOF component of the anomalous zonal mean quantities. When the SAPAs are positive (negative) in the northern hemisphere, they are negative (positive) in the southern hemisphere. Large values of SAPAs are usually observed in mid- and high-latitude areas in all but the solstice seasons. In boreal summer and winter, relatively stronger perturbations of IHO-related SAPA are found in the Asian monsoon region, which shows a large difference from the status in boreal spring and fall. This suggests that seasonal mean monsoon activity is globally linked via air mass redistribution globally on interannual timescales, showing a very interesting linkage between monsoons and the IHO in the global domain. In all seasons, large values of SAPA always exist over the Antarctic and the surrounding regions, implying a close relation with Antarctic oscillations.

Key words: inter-hemispheric oscillation, seasonality, interannual variability, surface air pressure anomaly

Citation: Guan, Z. Y., C. H. Lu, S. L. Mei, and J. Cong, 2010: Seasonality of interannual inter-hemispheric oscillations over the past five decades. *Adv. Atmos. Sci.*, **27**(5), 1043–1050, doi: 10.1007/s00376-009-9126-z.

1. Introduction

The low-frequency variability of atmospheric mass redistribution bears an intimate relation to global climate change, to which many scientists worldwide have paid more and more attention (IPCC, 1990; Keeling and Shertz, 1992; Hurrell, 1995; Shindell et al., 1999). Thompson and Wallace (1998) made an EOF analysis of boreal sea-level pressure, arriving at an Arctic oscillation (AO) mode, which shows a close relationship with the North Atlantic Oscillation (NAO, see e.g. Hurrell, 1995). Subsequently, Gong and Wang (1999) discovered a zonally symmetrical barotropic mode at southern extratropical latitudes, referred to as Antarctic Oscillation (AAO). Both the AO and AAO show scenarios of large-scale air mass redistribution with well defined patterns in the bi-hemispheric extratropical and polar regions. These two oscillations have been found to be related to many climate phenomena in different parts of the world (Rothrock et al., 1999; Serreze et al., 2000; Qin et al., 2005), and are confined to a hemispheric scale.

However, disturbances with scales larger than a hemisphere should also be captured in surface air pressure data. This is because inter-hemispherically interrelated weather and climate features occur, owing to the inhomogeneous solar heating that drives atmospheric mass, angular momentum, and energy into

*Corresponding author: GUAN Zhaoyong, guanzy@nuist.edu.cn

the opposite hemisphere. For example, when the winter hemisphere experiences an ascent of average pressure due to cooling, the opposite occurs in the summer hemisphere (Chen et al., 1997) and the signal is even detected in the earth's deformation sounding signal (Blewitt and Lavallee, 2001). An analysis of daily surface air pressure (SAP) demonstrates that air mass exchange does extend from one hemisphere to the other across the equator (Baldwin, 2001). Further, it is found that when the sea ice area increases in one hemisphere, it decreases in the other (Xie and Bao, 1995). The above cited research suggests the possible inter-hemispheric linkage of atmospheric disturbances between the northern and southern hemispheres. Guan and Yamagata (2001, GY01 hereafter), examined air mass redistributions on the global scale, showing opposing increases/decreases in one hemisphere with respect to the other (Fig. 1), and coined this phenomenon as the Inter-Hemispheric Oscillation (IHO). Note that the area-weighted surface air pressure anomalies averaged over the global domain show a decreasing trend from 1958 to 2006, presumably supporting the hypothesis of conservation of global air mass.

GY01 made an analysis of IHO variations on interannual time scales as illustrated in Fig. 1, based on monthly data. Recently, the seasonal cycle of inter-hemispheric exchanges of air mass based on multi-year mean data has also been discussed (Lu et al., 2008), interestingly demonstrating that seasonal changes of water vapor content in the atmosphere play a very important role in driving dry air from one hemisphere to another. However, the seasonally stratified IHO features on interannual time scales have still remained unexamined. In the present article, we will explore the interannual IHO patterns in different seasons.

2. Data and Methods

2.1 *Data*

The NCEP/NCAR monthly mean reanalysis (Kalnay et al., 1996) from January 1958 through December 2006 (totally 588 months) is used in the present article. Variables analyzed include surface air pressure (SAP, p_s) and 17-layers of geopotential height (H) data from 1000–10 hPa on a 2.5°×2.5° grid. The other two reanalysis datasets employed herein are ERA40 from 1958 through to 2001 (Uppla et al., 2005) and JRA25 (Onogi et al., 2007) from 1979 through to. Because the interannual variability of globally averaged water vapor pressure is much smaller than that of p_s (Lu et al., 2008) and the total variance of globally averaged anomalous vapor pressure at the earth surface accounts only for 5% of the variance of global mean SAP anomalies (Fig. 1), the departure from conservation of global air mass shown in Fig. 1 is likely to result from data assimilation (Guan and Yamagata, 2001). Note that all data have been preprocessed by removing the long term trends from the time series of each physical quantity. To clarify the differences of the interannual IHO in one season versus another, the analyses in the present work are seasonally stratified.

2.2 *Methods*

The inter-hemispheric total air mass has a prominent interannual anomaly signal that displays a see-saw pattern (Fig. 1), so that according to GY01, a roughly oscillatory index can be constructed for the Northern Hemisphere (NH) and Southern Hemisphere (SH) as

$$\begin{aligned} I_{\mathrm{IHO}} &= p_{\mathrm{sNH}} - p_{\mathrm{sSH}} \\ p_{\mathrm{sNH}} &= \int_0^{\frac{\pi}{2}} \bar{p}_s \cos\varphi d\varphi \end{aligned}, \tag{1}$$

where p_{sNH} and p_{sSH} represent, respectively, the areally weighted averages of anomalous SAP for the boreal and austral hemispheres, while $\bar{p}_s$ represents the zonal mean surface air pressure anomaly, and φ is the latitude .

EOF- and regression-based analysis techniques are employed to obtain the IHO patterns. In conducting the EOF analysis, the grid point values are multiplied by an area weighting factor, which is the cosine of the latitude.

3. Results

3.1 *Inter-hemispheric oscillation index and its variance in the different seasons*

The variance of IHO index shows roughly the intensity of the inter-hemispheric redistributions of air mass. It is seen from Table 1 that the IHO is strongest in boreal winter (index= 0.304) rather than in other

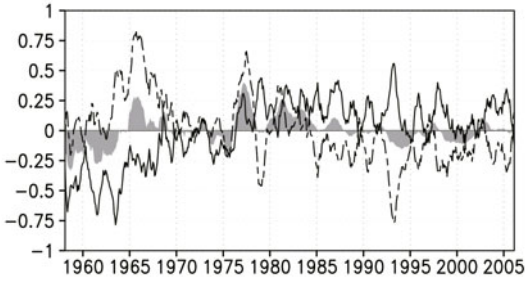

Fig. 1. Areally weighted mean surface air pressure (hPa), which has been smoothed with an 11-month window, with shading for the global results, and a solid (dashed) line for the northern (southern) hemisphere results.

Table 1. Variance of seasonal IHO index as derived from NCEP-NCAR reanalysis and the related correlations of IHO index from NCEP with that from ERA40 for period 1958–2001, and with that from JRA25 for period 1979–2006.

	Variance	Correlation coefficient	
		NCEP-ERA40	NCEP-JRA25
Winter	0.304	0.870	0.909
Spring	0.246	0.841	0.893
Summer	0.267	0.712	0.883
Autumn	0.264	0.803	0.851

seasons. As compared to the IHO variance in equinox seasons, the IHO appears stronger in solstice seasons. Lu et al. (2008) discussed that the seasonal cycle of the inter-hemispheric air mass flux shows a pronounced seesaw structure in the troposphere, especially in solstice seasons, and this is climatologically related to the Asian monsoons. The variance as shown in Table 1 also implies that the Asian monsoons possibly play an important role in the inter-hemispheric exchange of air mass. Note that the seasonal IHO index (I_{IHO}) derived from NCEP/NCAR, ERA40, and JRA25, as shown in Fig. 2 with time series, indicates the consistency of the evolution; i.e., the IHO indices experience close interannual variations and similar amplitudes to one another, particularly after the late 1980s. Especially noted is that the 1958–2001 IHO indices from NCEP and ERA40 maintain a significant correlation. Also, the correlation coefficient in summer is the smallest (0.71) out of all the seasons (Table 1). Because of the consistency of the three datasets for the IHO index (Fig. 2) and the long period of the data record, we use the NCEP/NCAR reanalysis for further examination of IHO features.

3.2 *IHO pattern*

The spatial distribution of seasonal IHO in anomalous SAP fields are presented in Fig. 3 for positive phases of seasonal I_{IHO} using the composite analysis. The large seasonal anomalies are mainly found in the extra-tropics in both the southern and northern hemispheres, especially in Eurasia, the Aleutian area, and the Antarctic region. These large anomalies are oppositely signed between the two hemispheres. These show the signature of the IHO as discussed in GY01 (2001).

The areas and values of the positive or negative anomalies of air mass vary from one season to another, showing the strong seasonalities of the interannual IHO (Fig. 3). Larger positive values are observed in the northern polar region while negative values are observed in the southern polar region. More interestingly, in the solstice seasons, the inter-hemispheric oscillations seem to occur between the polar regions and the extratropics. During boreal winter, there exist positive anomalies in the Arctic region and at the high latitudes of Eurasia and the north American continent, while large negative values prevail in the southern hemisphere, especially in the tropical ocean regions from the south Atlantic eastward to the western Pacific (Fig. 3a). During boreal summer, lager positive anomalies of air mass are seen in both high latitudes and the Asian–Australian monsoon regions while nega-

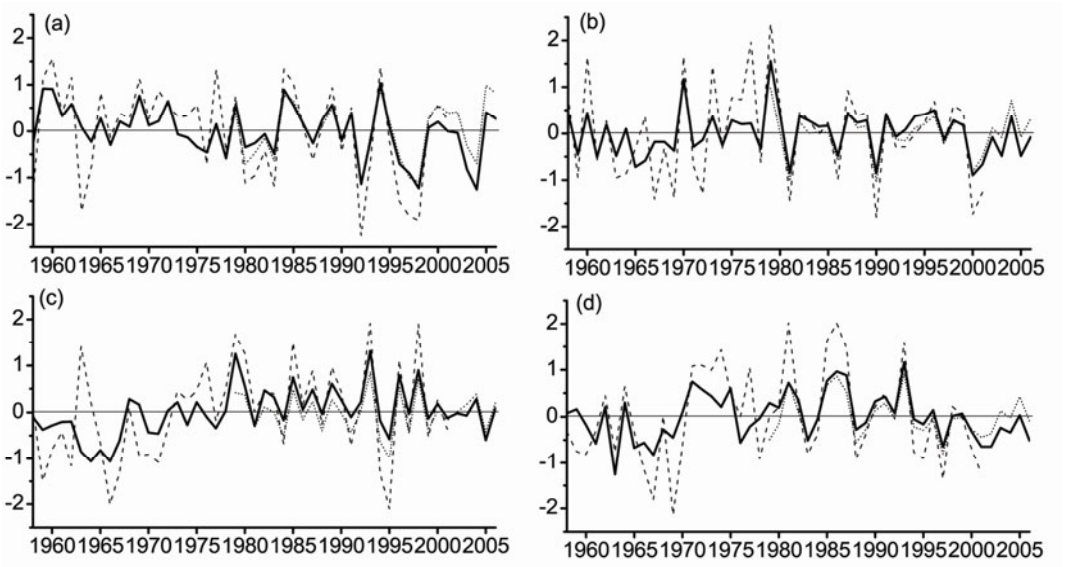

Fig. 2. I_{IHO} from NCEP (solid line), ERA40 (dashed), and JRA25 (dotted), for (a) winter, (b) spring, (c) summer, and (d) autumn.

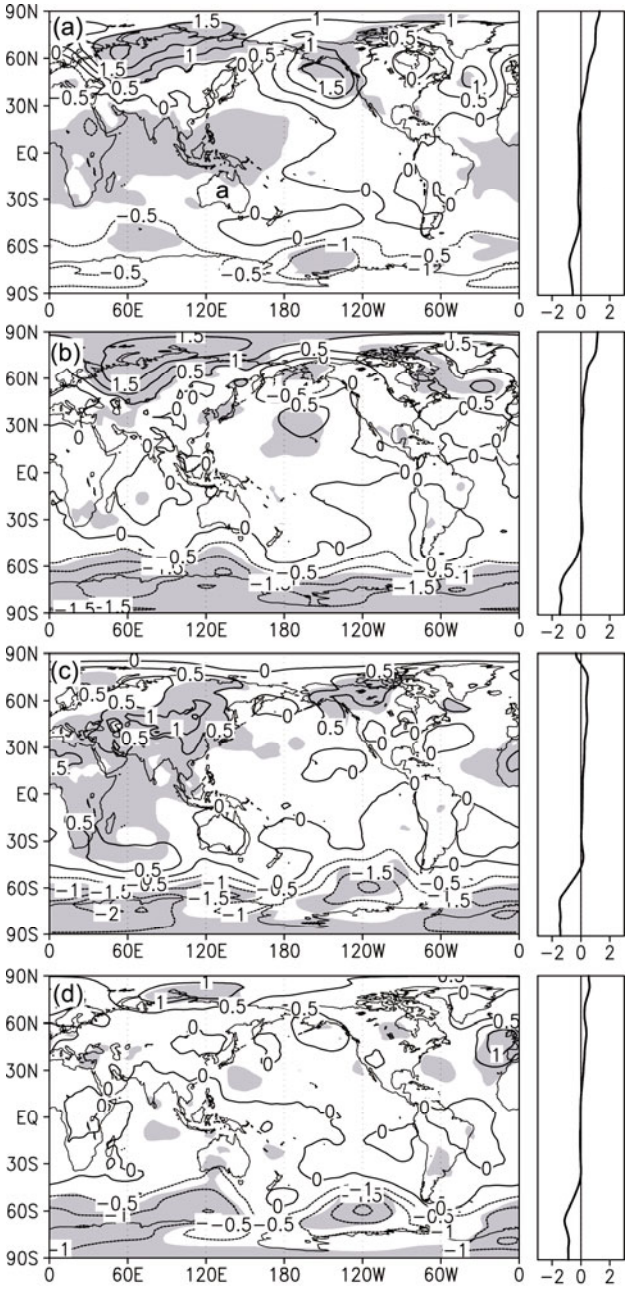

Fig. 3. Composites of global (left) and zonal mean (right) surface air pressure anomalies for positive I_{IHO} years. The contour interval is 0.5 hPa, with the shading for significance above 95% confidence level: (a) winter, (b) spring, (c) summer, and (d) autumn.

tive anomalies are found in the Antarctic regions (Fig. 3c). All these results as displayed in Fig. 3 demonstrate the intrinsic global patterns of the IHO. In view of the fact that strongly positive SAP zones in boreal summer are largely confined to 30°S–60°N of the eastern hemisphere, SAP variation determines, to great degree, the surface wind field (Murphree and Van Den Dool, 1988). As monsoons are dominantly active in the eastern Hemisphere, the IHO seasonal differences are apparently associated with anomalous monsoons.

Lu and Guan (2009) examined the simultaneous relationships of springtime IHO with climate of China, showing the good relationship between the IHO and occurrences of dust storms in northern China. In the present work, it is worth noting that there are always bigger negative anomalies of air mass at southern extratropical latitudes in each of the seasons, particularly in southern summer, and the noticeable northern air mass pile-up happens especially in winter, which is potentially related to wintertime extreme cold temperature in the extratropics of the winter hemisphere.

3.3 *Redistribution of zonal mean air mass anomalies*

To further investigate the principal patterns and variations of globally anomalous air mass distribution for different seasons, an EOF analysis is performed on zonal mean SAP ($\bar{p}_{\mathrm{s}}$) anomalies for each season. As in GY01, we define $h_n(t), R_n(\varphi), \mu(=\cos\varphi)$ as the time coefficient of the nth eigenvector, the eigenvector, and areal weighting factor, respectively. Then $\bar{p}_{\mathrm{s}}$ can be given as

$$\overline{p_s} = \sum_{n=1}^{\infty} h_n(t) R_n(\varphi)/\mu \,. \tag{2}$$

From (1) and (2), we redefine I_{IHO} as

$$I_{\mathrm{IHO}} = \sum_{n=1}^{\infty} h_n(t)(R^*_{n\mathrm{NH}} - R^*_{n\mathrm{SH}}) \,. \tag{3}$$

In Eq. (3), $R^*_{n\mathrm{NH}} - R^*_{n\mathrm{SH}}$ denotes the difference of anomalous air pressure averaged over the Northern Hemisphere from that over the southern Hemisphere for the nth eigenvector. Equation (3) shows that the IHO, being simply represented by an index as defined in Eq. (1), consists of many components as obtained from EOF analysis. Table 2 shows the contribution of EOF1 to the total variance of zonal mean surface air pressure anomalies, along with the correlation coefficients of EOF1 with the IHO index as defined by Eq. (1). It is seen from Table 2 that the leading EOF in boreal winter explains 37% of total variance of the SAP anomalies. However, the correlation of the time series of coefficients of EOF1 with IHO index is too small to be neglected. This is because the AO and AAO are the dominant modes in boreal winter (Fig. 4a). EOF1 is just the component for the AO and the simultaneous AAO as seen in Fig. 4a. From Table 2 and Fig. 4 it is seen that the principal patterns (EOF1) of air mass

Table 2. Contributions of EOF1 to the total variance of seasonal mean air pressure anomalies and the correlation coefficient of EOF1 with IHO index. The numbers with asterisks denote values statistically above the 95% confidence level using a t-test.

	Variance contribution (%)	Correlation coefficient
Winter	37	0.06
Spring	39	0.49*
Summer	56	0.70*
Fall	42	0.32*

anomalies differ significantly from one season to another. In spring and summer the correlations between the time series of the coefficients of the first EOF component and I_{IHO} reach 0.49 and 0.70, respectively. The anomalous accumulation of air mass differs greatly between the two hemispheres ($R^*_{1\mathrm{NH}} - R^*_{1\mathrm{SH}}$), exhibiting a very pronounced IHO signature. Additionally, the values of both $R^*_{1\mathrm{NH}}$ and $R^*_{1\mathrm{SH}}$ change greatly from one season to another although the AO and AAO signatures are seen in the zonal mean EOF1 patterns. These scenarios of IHO seem to be consistent with those results as observed in Fig. 3. However, as the IHO signal is indeed found in winter as displayed in Fig. 3a, it is believed that the first leading EOF mode of zonal mean SAP anomalies is unable to show the IHO signature in boreal winter.

3.4 *IHO vertical structure in different seasons*

As the SAP anomalies are intrinsically related to the geopotential height variations in the vertical direction from the earth surface to the top of the atmosphere, the zonal mean height anomalies (H') in

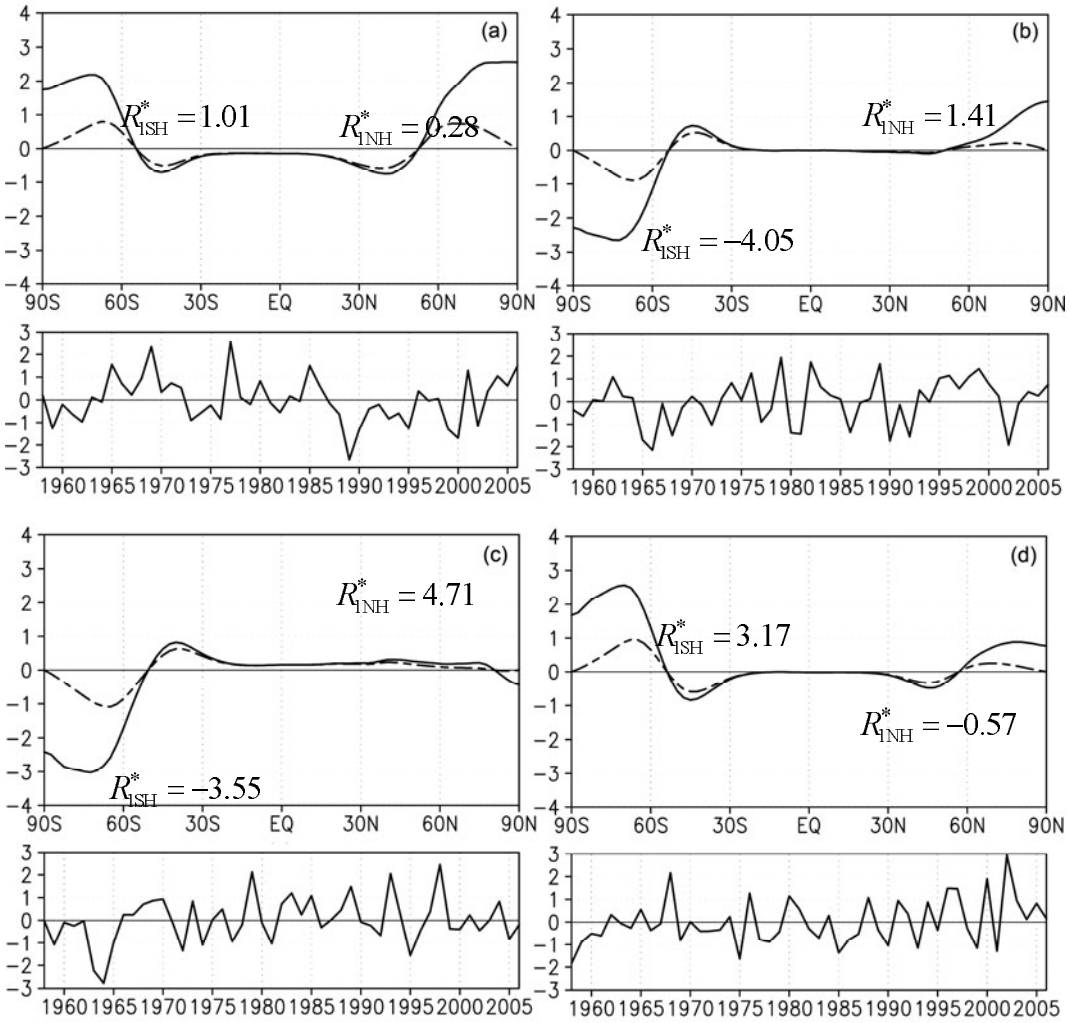

Fig. 4. R_1 (EOF1, dashed line, upper panel), R/μ (solid line, upper panel), and the corresponding temporal coefficient (lower panel), for (a) winter, (b) spring, (c) summer, and (d) autumn.

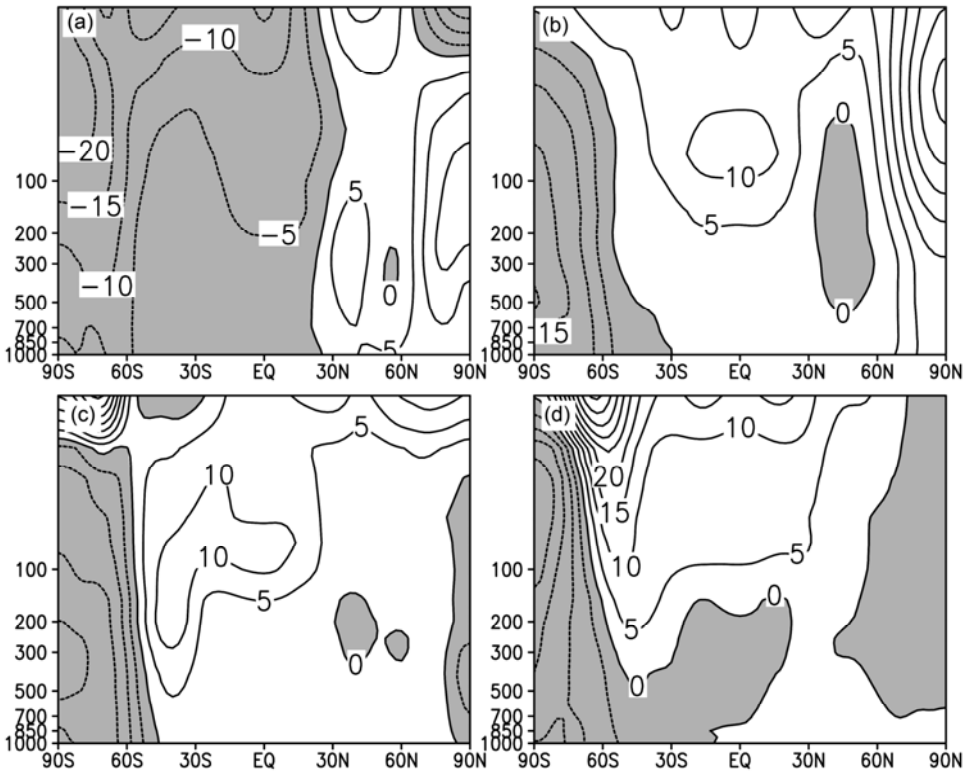

Fig. 5. Results of geopotential heights regressed upon I_{IHO}, contoured at 5 gpm, for (a) winter, (b) spring, (c) summer, and (d) autumn.

a season are regressed upon the standardized I_{IHO} of the same season to obtain the vertical structure of IHO-associated height disturbances (Fig. 5). It is seen from Fig. 5 that the anomalous geopotential height projected upon a corresponding I_{IHO} yields high-valued zones in the middle and high latitudes, in agreement with results from earlier composites and EOF approaches (Figs. 3 and 4). In boreal winter and spring (Figs. 5a and 5b), there are large values in the polar regions, suggesting a barotropic structure of IHO. But in boreal summer and fall, the large positive values of height anomalies are found over the southern extratropics in middle and upper parts of the troposphere, along with large negative values in the Antarctic from the troposphere upward to the mid-upper stratosphere. These features are roughly the signatures of the AAO. However, distinctive IHO signatures are clearly visible from the earth surface up to the mid-troposphere.

3.5 *Further examining IHO signatures in SAP anomalies*

The correlation coefficients between the seasonal IHO index and surface air pressure anomalies (SAPA) are presented in Fig. 6 to investigate IHO signatures in more detail. It is apparent that there is a correlation between I_{IHO} and SAPA over most of the globe, with positive (negative) correlations prevailing in the boreal (austral) hemisphere and high negative correlations over the Antarctic for all seasons. The positive correlations are dominant in Europe, the eastern North Pacific, and Alaska and appreciable negative correlations also emerge in the tropical Indian Ocean, East Asia, and the tropical western Pacific in addition to the Antarctica region in boreal winter, perhaps in association with inter-hemispheric air mass exchange caused by the surge of southeast Asian SAP in winter (Carrera and Gyakum, 2003). In spring the high positive correlations are found in different regions: over extratropical Eurasia, eastern Canada, and the North Atlantic. It is noteworthy that high positive correlations are found in China in the Yangtze-Huaihe River valleys, in agreement with results from the analysis of station data (Lu and Guan, 2009). In summer the significant correlation zones are maximized in scope, with high positive correlations covering nearly all of Asia, Africa, and Europe, the Indian Ocean, and western North America, as well as the tropical western Pacific, while high negative correlations are spread from Antarctica to 55°S and further northward in the southern hemisphere. In autumn these high correlation zones shrink in area, with positive high correlations situated be-

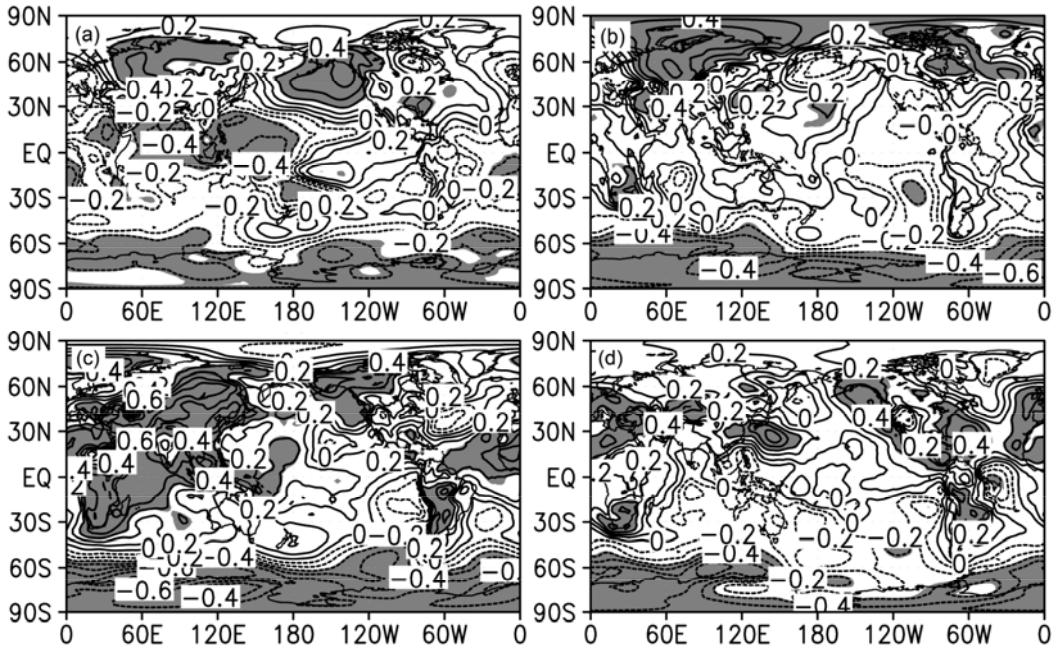

Fig. 6. Correlations of I_{IHO} with SAPA. The contour interval is 0.1, with shading indicating significance above the 95% confidence level using a t test. (a)–(d) are for winter, spring, summer, and autumn, respectively.

tween 30°–60°N, except for the central-eastern North Pacific.

4. Conclusions and discussions

The seasonality of interannual IHO variations has been examined for the period 1958–2006 by using NCEP/NCAR reanalysis of both monthly mean surface air pressure and geopotential height fields. It has been found that there is a distinct seesaw behavior in all four seasons between the northern and southern hemispheres in both the composites of SAPA and the leading EOF component of the anomalous zonal mean quantities. The IHO signature is observed with relatively larger perturbations of SAPA in mid- and high-latitude areas of each hemisphere in boreal winter, spring, and fall. When the IHO is in its positive phase, the SAPA is positive in the northern hemisphere and negative in the southern hemisphere. When the IHO is in the negative phase, the scenario is oppositely signed. It is revealed that the relatively stronger perturbations of IHO-related SAPA perturbations move geographically southward from high latitudes to extratropical regions with seasonal changes. For example, in boreal summer an IHO signature is very clearly seen between the Asian monsoon and Antarctic regions. This is quite different from the scenarios in other seasons. In all four seasons, the IHO signature in the vertical in the troposphere as detected from the regressions of geopotential height anomalies onto I_{IHO} looks similar to that for SAPA. As the interannual IHO is defined from SAPA (Guan and Yamagata, 2001), the IHO signature can be exhibited more clearly in correlations of SAPA with the IHO index. The surface air pressure anomalies decrease (increase) always mainly in the Antarctic region, which has almost nothing to do with the seasonal changes which are occurring, whereas the anomalies increase (decrease) in different regions in the northern hemisphere in different seasons. The surface air pressure anomalies change largely in the Asian monsoon region from one season to another in association with the IHO, showing that the seasonal mean monsoon activities are globally linked via the air mass redistribution on interannual timescales.

It should be noted that the mechanisms for formation of both the IHO and its seasonality have not been clarified yet. As seen in Figs. 3–6, the regions with large variances of the IHO are distributed mainly in the middle and high latitudes (except for the Northern Hemisphere in summer). This phenomenon is likely to be theoretically related to Rossby waves. This is probably because of the zonal-mean zonal wind perturbations. Zonal-mean zonal wind variations may alter the Coriolis force longitudinally, and hence modify the pressure gradient force (Fig. 5) to bring about a redistribution of air mass. Furthermore, the zonal inhomogeneity of air pressures is marked by intense locality (Fig. 3) that may be associated with inten-

sity changes of the atmospheric centers of action or quasi-steady circulations. Despite the fact that Rossby waves moves relatively faster, the linkage between IHO interannual variation and Rossby wave activity can be established from the atmospheric response to anomalous heat sources or the long-term averaged effect of dynamic processes inside the atmosphere. It is worth noting that high values of IHO-related air mass anomalies are always existent in middle and high latitudes in the southern hemisphere in all four seasons. We have examined the relationship between IHO and AAO, and find that the IHO index (Guan and Yamagata, 2001) is well correlated with the AAO index (Gong and Wang, 1999) in all seasons. These suggest that the IHO is probably closely related to the AAO. Therefore, what are the physical relations between these phenomena, as well as with Rossby waves? These questions deserve to be answered in the future.

Acknowledgements. This work is supported jointly by the National Key Technology R&D Program (Grant No. 2007BAC29B02), the National Natural Science Foundation of China (NSFC, Grant No. 40675025), and the Key Laboratory of Meteorological Disasters, Nanjing University of Information Science & Technology (NUIST, KLME060101). The NUIST Center of Atmospheric Data Service under the Geoscience Division of NSFC provided data through their service. All figures in the present article were made using the Grads suite of software.

REFERENCES

Baldwin, M. P., 2001: Annular modes in global daily surface pressure. *Geophys. Res. Lett.*, **28**, 4115–4118.

Blewitt, G., and D. Lavallée, 2001: A new global mode of earth deformation: Seasonal cycle detected. *Science*, **294**, 2342–2345.

Carrera, M. L., and J. R. Gyakum, 2003: Significant events of interhemispheric atmospheric mass exchange: Composite structure and evolution. *J. Climate,* **16**, 4061–4078.

Chen, T. C., J. M. Chen, S. Schubert, and L. L. Takacs, 1997: Seasonal variation of global surface pressure and water vapor. *Tellus*, **49**A, 613–621.

Gong, D., and S. Wang, 1999: Definition of Antarctic Oscillation Index. *Geophys. Res. Lett.*, **26**, 459–462.

Guan, Z., and T. Yamagata, 2001: Interhemispheric oscillations in the surface air pressure field. *Geophys. Res. Lett.*, **28**, 263–266.

Hurrell, J. W., 1995: Decadal trends in the North Atlantic Oscillation: Regional temperatures and precipitation. *Science*, **269**, 676–679.

IPCC, 1990: *Climate Change*: *The Scientific Assessment.* Cambridge University Press, 365pp.

Kalnay, E., and Coauthors, 1996: The NCEP-NCAR 40-Year Reanalysis Project. *Bull. Amer. Meteor. Soc.*, 77, 437–471.

Keeling, R. F., and S. R. Shertz, 1992: Seasonal and interannual variations in atmospheric oxygen and implications for the global carbon cycle. *Nature*, **358**, 723–727.

Lu, C. H., and Z. Y. Guan, 2009: On the interannual variation in spring atmospheric inter-hemispheric oscillation linked to simultaneous climate in China. *Progress in Natural Sciences*, **19**, 1125–1131.

Lu, C. H., Z. Y. Guan, S. L. Mei, and Y. J. Qin, 2008: Seasonal cycle of atmospheric mass interhemispheric oscillation. *Chinese Science Bulletin,* **53**, 3226–3234.

Murphree, T., and H. Van Den Dool, 1988: Calculating tropical winds from time mean sea level pressure fields. *J. Atmos. Sci.*, **45**, 3269–3282.

Onogi, K., and Coauthors, 2007: The JRA-25 reanalysis. *J. Meteor. Soc. Japan,* **85**, 369–432.

Qin, J., P. Wang, and Y. Gong, 2005: Impacts of Antarctic Oscillation on summer moisture transport and precipitation in Eastern China. *Chinese Geographical Science*, **15**, 22–28.

Rothrock, D. A., Y. Yu, and G. A. Maykut, 1999: Thinning of the Arctic sea-ice cover. *Geophys. Res. Lett.*, **26**, 3469–3472.

Serreze, M. C., and Coauthors, 2000: Observational evidence of recent change in the Northern high-latitude environment. *Climatic Change*, **46**, 159–207.

Shindell, D., D. Rind, N. Balachandran, J. Lean, and P. Lonergan, 1999: Solar cycle variability, ozone, and climate. *Science*, **284**, 305–308.

Thompson, D. W. J., and J. M. Wallace, 1998: The Arctic Oscillation signature in the wintertime geopotential height and temperature fields. *Geophys. Res. Lett.*, **25**, 1297–1300.

Uppala, S. M., and Coauthors, 2005: The ERA-40 reanalysis. *Quart. J. Roy. Meteor. Soc.*, **131**, 2961–3012.

Xie, S. M., and C. L. Bao, 1995: Interrelation in sea ice area between the North and South Poles. *Chinese Science Bulletin,* **40**, 632–635. (in Chinese)